



HAL
open science

Influence of Bonding Delaminations on The Electromechanical Admittance (EMA) of a Single-element Piezoelectric Transducer

Wenxiang Ding, Maxime Bavencoffe, Marc Lethiecq

► **To cite this version:**

Wenxiang Ding, Maxime Bavencoffe, Marc Lethiecq. Influence of Bonding Delaminations on The Electromechanical Admittance (EMA) of a Single-element Piezoelectric Transducer. Forum Acusticum, Dec 2020, Lyon, France. pp.2857-2862, 10.48465/fa.2020.0479 . hal-03240269

HAL Id: hal-03240269

<https://hal.science/hal-03240269>

Submitted on 30 May 2021

HAL is a multi-disciplinary open access archive for the deposit and dissemination of scientific research documents, whether they are published or not. The documents may come from teaching and research institutions in France or abroad, or from public or private research centers.

L'archive ouverte pluridisciplinaire **HAL**, est destinée au dépôt et à la diffusion de documents scientifiques de niveau recherche, publiés ou non, émanant des établissements d'enseignement et de recherche français ou étrangers, des laboratoires publics ou privés.

Influence of Bonding Delaminations on the Electromechanical Admittance (EMA) of a Single-element Piezoelectric Transducer

Wenxiang DING¹ Maxime BAVENCOFFE¹ Marc LETHIECQ¹

¹ GREMAN UMR-CNRS 7347, Université de Tours, INSA Centre Val de Loire, Blois, France
Email: wenxiang.ding@insa-cvl.fr

ABSTRACT

The objective of this work is to determine procedures to monitor the behavior of a single-element probe during its lifetime and detect degradations before they significantly affect the performance of the system. To achieve this, an electromechanical admittance (EMA) based method is envisaged numerically and experimentally. A simplified single-element transducer consisting of a piezoceramic disc, a bonding layer and a backing is studied and the influence of bonding delaminations on EMA is investigated. First, a numerical model based on the finite element method is developed and the effect of three different types of delaminations are analyzed by two- (2D) and three-dimensional (3D) modelling. Secondly, transducers with different shapes of 3D printed backings are mounted and experiments are conducted using an impedance analyzer. Experimental results are found to be in good agreement with numerical solutions and it shows that changes in EMA can particularly reveal the occurrence and extent of delamination in an ultrasound probe.

1. INTRODUCTION

The transducer is an important part of any ultrasonic instrumentation system used for applications such as medical diagnostics and non-destructive evaluation (NDE). However, misuse, such as dropping, and the ageing process can cause breakages in cables or components, delamination between different layers and cracked crystal [1, 2]. Defects within the active element, backing or other constitutive elements, loss of adhesion between layers can significantly waken the performance of the system. This emphasizes the need to periodically monitor the transducer characteristics during its lifetime and detect any damage that could appear.

Early methods used for ultrasound transducer fault detection are mainly based on image quality inspection, such as tissue-mimicking phantom measurements [3] and electrical tests [1]. These measurements, testing either in phantom or water, rely on the transmit-receive response of the transducer and are equipment-reliant and time-consuming. Recently, a method using the in-air reverberation pattern generated from transducer operating in air is presented and shows a good potential [4]. In this work, an electromechanical admittance-based (EMA-based) method is proposed to monitor the behavior of the transducer during its lifetime.

Simplified from traditional multi-element ultrasound probe, a single-element transducer consisting of a piezoelectric disc, a bonding layer and a backing is studied numerically and experimentally. Firstly, an approximate simulation of delamination is introduced into the traditional one-dimension (1D) KLM model to explore the influence of delamination on EMA. Then a more accurate numerical model based on the finite element (FE) method is built and its accuracy is validated by comparison with KLM model. After that, the influence of three specific different types of bonding delaminations on EMA is investigated based on the FE model built. Finally, transducers with different shapes of 3D printed backings are mounted and measured experimentally and their results are compared with ones from FE model and discussed.

2. EQUIVALENT CIRCUIT

Methods for studying the characteristic of transducer and simulating wave propagation have been widely explored. The most commonly used methods are mechanical and equivalent electrical circuits, such as the KLM model [5], and finite elements.

2.1 Components and materials

The simplified single-element transducer is composed of a piezoceramic disc and a 3D printed polylactic acid (PLA [6]) backing. They are bonded by an acoustic coupler phenyl salicylate (SALOL [7]), which melts at 42 °C. The diagram is shown in Fig. 1.

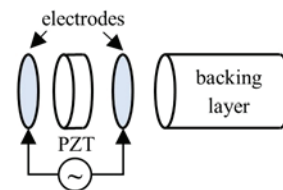


Figure. 1. Diagram of the simplified transducer

The soft piezoelectric material PZ27 (Ferroperm™ Piezoceramics [8]) is used here, with diameter of 16mm and central frequency of 1.76MHz. Thickness (t), density (ρ), elastic (c_{ij}^E), piezoelectric (e_{kj}) and dielectric constants (ϵ_{kk}^S) shown in Tab. 1 are based on the datasheet provided by the manufacturer. $\delta_{c_{33}^E}$ and $\delta_{\epsilon_{33}^T}$ indicate the mechanical and dielectric loss factors.

Geometry and material data of passive elements, *i.e.* bonding and backing layer, are shown in Tab. 2. c_L and c_S are the velocity of longitudinal and transverse waves, δ_m

indicates the isotropic loss factor. The acoustic impedance of the PLA material is around 2.9 MRayl. Similar backing materials are widely used to improve the bandwidth but also maintain a good sensitivity of transducer.

PZ27 Ceramic						
t	ρ	c_{11}^E	c_{12}^E	c_{13}^E	c_{33}^E	c_{44}^E
(mm)	(kg/m ³)	(GPa)	(GPa)	(GPa)	(GPa)	(GPa)
1.13	7879.5	147.4	104.9	93.7	112.6	23
e_{31}	e_{33}	e_{15}	$\epsilon_{11,r}^S$	$\epsilon_{33,r}^S$	$\delta_{c_{33}}^E$	$\delta_{e_{33}}^T$
(C/m ²)	(C/m ²)	(C/m ²)			(%)	(%)
-3.09	16.03	11.64	1129.7	913.7	1.35	1.7

Table 1. Geometry and material data of the PZ27 layer

PLA backing				
t	ρ	c_L	c_S	δ_m
(mm)	(kg/m ³)	(m/s)	(m/s)	(%)
20	1200	1825.8	919.7	5
Salol Bonding layer				
t	ρ	c_L	c_S	δ_m
(mm)	(kg/m ³)	(m/s)	(m/s)	(%)
0.09	1250	2369	994	1

Table 2. Geometry and material data of backing and bonding layer

2.2 KLM model

The KLM model [5] is a 1D equivalent circuit model to represent the behavior of the transducer when only one resonant mode is considered.

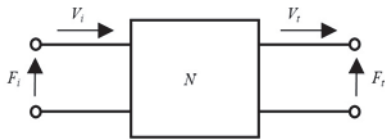


Figure 2. Quadrupole representation of a single-element transducer

Regarding the backing layer and back acoustic port as an internal network, the whole transducer and the load medium can be represented by a quadrupole system, as shown in Fig. 2, where F_i , V_i indicate the voltage and current of the electric port, F_t , V_t indicate the force and velocity of the mechanical port, and N indicates the transfer matrix of the system.

The electrical admittance at the electric port is:

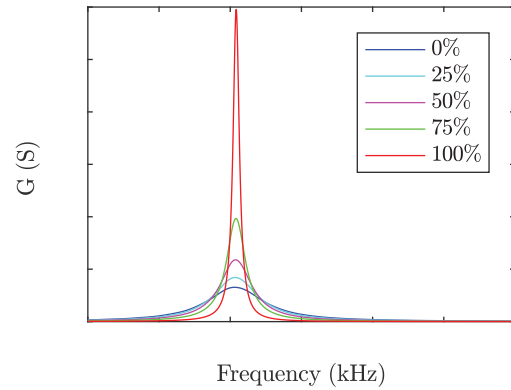
$$Y(\omega) = \frac{V_i(\omega)}{F_i(\omega)} = \frac{N_{11} - N_{21}Z_t}{N_{22}Z_t - N_{12}} \quad (1)$$

where Z_t is the front load mechanical impedance and is equal to F_t/V_t .

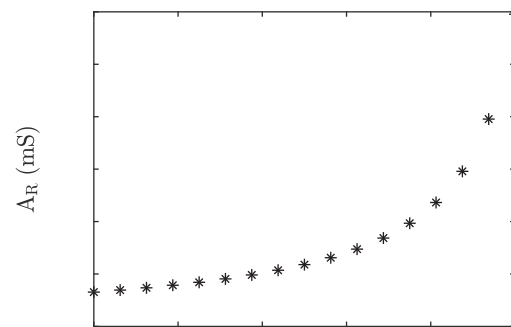
To simulate a delamination through KLM model, the area of the bonding layer is modified, resulting in a change in its mechanical impedance and a variation in its transfer matrix. The delamination ratio (Δ), defined as in Eqn. (2), shifts from 0% (intact) to 100% (no backing).

Assuming that the transducer is surrounded by air, Fig.3

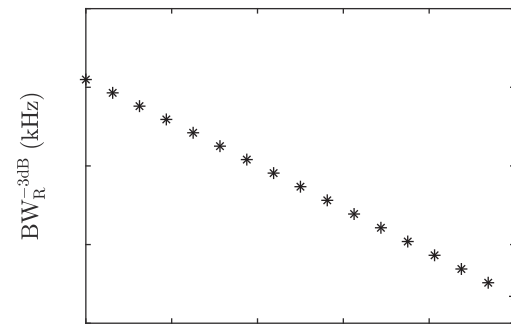
$$\Delta = \frac{\text{delamination area}}{\text{cross-sectional area}} \times 100\% \quad (2)$$



(a)



(b)



(c)

Figure 3. Delamination influence on EMA based on KLM model: (a) conductance, (b) resonance amplitude, (c) -3dB bandwidth.

presents the influence of delamination on EMA. Geometry and materials parameters are shown in Tab.1 -2. Results based on KLM show that as Δ increases, the resonance peak becomes shaper and higher (Fig. 3(a)), which leads to the growth of the resonance amplitude A_R (Fig. 3(b)) and the decrease of the -3dB bandwidth BW_R^{-3dB} (Fig. 3(c)). The BW_R^{-3dB} here is equal to the bandwidth at frequencies corresponding to $G_{max}/\sqrt{2}$. We can see that indicators extracted from EMA, *i.e.* A_R or BW_R^{-3dB} changes monotonically with Δ . This demonstrates that if we take

the intact transducer (0%) as a reference state, the increase in A_R and decrease in BW_R^{-3dB} from one test session to another can be used to assess the occurrence and severity of a delamination.

3. FINITE ELEMENT MODELLING

The equivalent circuit model is efficient and accurate to a certain extent but is limited to one dimension and one mode. One dimension means that the specific feature of delamination, such as geometry (shape and position), cannot be characterized by the model and one mode means only the longitudinal vibration is considered, the other modes and the possible coupling effects are neglected. By contrast, FE model takes into account the radial vibration and the coupling effect between different modes of vibration. Although it takes some computational resource, FE model provides more realistic and accurate solutions and can also be applied to model more complex structures, such as multilayered ones with or without specific defects.

3.1 FE model

FE modeling has been carried out with COMSOL Multiphysics® software. The Electrostatics, Electrical Circuit and Solid Mechanics modules have been used. Fig. 4 presents the 2D axisymmetric FE model.

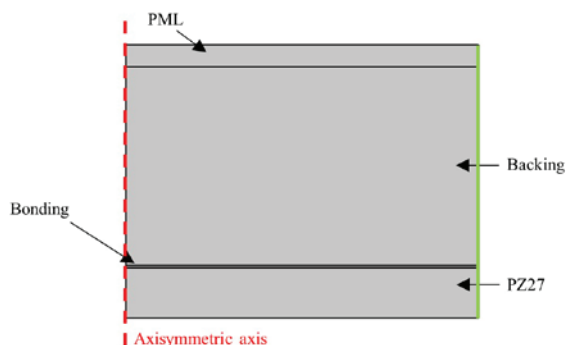


Figure. 4. 2D axisymmetric FE model.

All simulations are performed assuming the transducer is in vacuum since the loading effect of light fluid, such as air, on the vibration of transducer is negligible [9]. The mechanical boundary condition is free and a perfectly matching layer (PML) is added at the rear of the backing layer to absorb reflection waves.

A frequency domain study is then performed where the frequency is swept from 1.4MHz to 2.4MHz, *i.e.* in the range of the central frequency of the piezoelectric layer.

3.2 Validation

FE model takes all vibration modes into account, but it can also regress to 1D modelling like KLM, that is, it is possible to only consider thickness vibration with the addition of a roller boundary condition applied to the peripheral surface of the transducer (green line in Fig.4) to constrain its vibration in the radial direction.

With the same geometry and material constants as above, the conductance and susceptance of an intact

transducer is calculated separately by KLM and FE model. Results are shown in Fig. 5. To better illustrate results, curves around resonance peaks are magnified. Results for the two models are found to overlap and the discrepancy of A_R and BW_R^{-3dB} are $Y_A = 0.06\%$ and $Y_{BW} = 0.32\%$ respectively. This proves the accuracy of the built FE model.

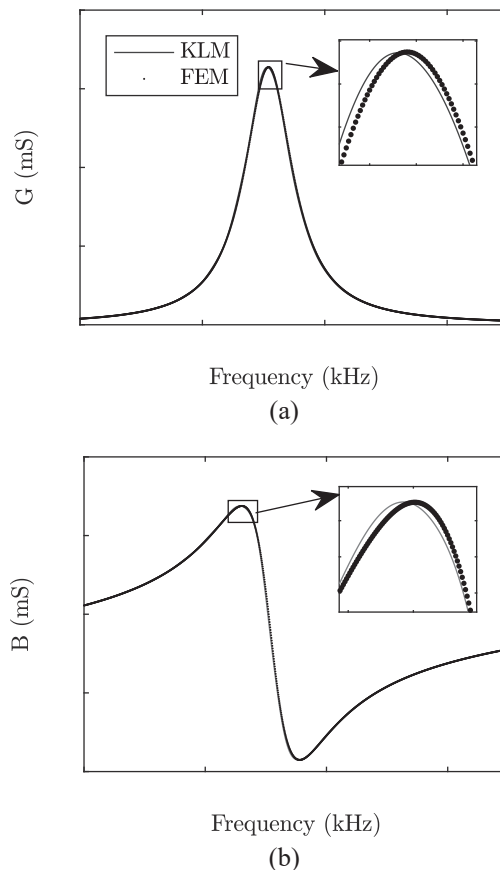


Figure. 5. Comparison between FE and KLM models: (a) conductance, (b) susceptance.

3.3 Delamination modelling

To study the influence of delamination on EMA, three different specific types of delaminations are considered, named as “center” (Fig. 6(a)), a circular delamination from the center of the disc towards the peripheric zone, “peripheric” (Fig. 6(b)), an annular delamination from the peripheric zone towards the center and “wedge” (Fig. 6(c)), a wedge-shaped delamination with a given angle, respectively.

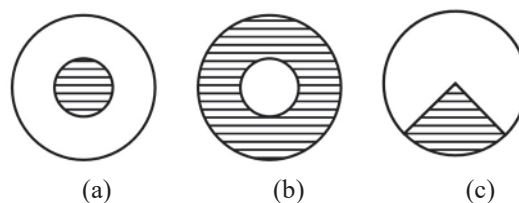


Figure. 6. Diagram of three types of delaminations: (a) center, (b) peripheric, (c) wedge.

As the three envisaged delaminations have different geometric symmetry, thus the first two kinds, *i.e.* “center”

and “peripheric”, are analyzed via 2D axisymmetric modelling with a total of 2016 rectangular quadratic Lagrange elements. As for the “wedge” delamination, it is evaluated by 3D symmetry modelling with a total of 288 prisms and 36000 hexahedra elements. The delamination ratio Δ changes in the same way as described in Eqn. (2).

4. EXPERIMENT VS SIMULATION

4.1 Experimental setup

The simplified single-element transducer is realized with soft PZT disc (Ferroperm PZ27 from Meggitt, Denmark) and a 3D printed PLA backing bonded by SALOL (see Fig. 7(a)).

Geometry and material constants have been given in Section 2, Tab. 1-2. A classical cylindrical backing with a diameter equal to that of the ceramic disc (Fig. 7(a)) as well as nine backings that correspond to the three types of delaminations with delamination ratios of 25%, 50% and 75% (see Fig. 7(b)) are printed and mounted. The admittance curves are measured by a HIOKI IM3570 impedance analyzer. The experimental setup is shown in Fig. 8.



Figure 7. Transducer components. (a) piezoceramic disc PZ27 and intact PLA backing; (b) nine 3D printed PLA backings.

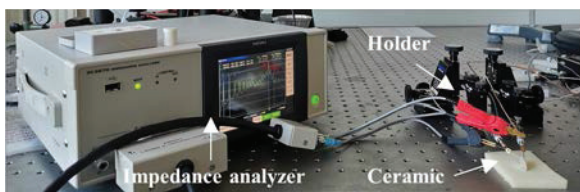


Figure 8. Measurement setup.

4.2 Loss factor measurements

As envisaged in §2.2, the influence of delamination on EMA curves is mainly reflected on the resonance amplitude and bandwidth. Actually, these features are also closely related to the losses of the transducer. Therefore, the determination of loss factors is critical to the analysis.

The mechanical and dielectric loss factors of PZ27 ceramic are measured based on theory proposed by Zhuang in [10]. Loss factors provided by manufacturer [8] in Tab. 1 are for c_{33}^E and ϵ_{33}^T and they are transformed into for c_{33}^D and β_{33}^S for comparison [11]. Discrepancy between the experimentally determined losses and the ones provided by manufacturer is shown in Tab. 3. We see that the experimental loss factors for c_{33}^D and β_{33}^S are much smaller than values provided by manufacturer’s datasheet.

Admittance curves calculated by FE model from these two sets of loss factor values are compared with experimental ones, as shown in Fig. 9. Tab. 4 illustrates the effect on EMA. We can see that when using measured loss factors, the difference on A_R between simulation and experiment is reduced from $Y_A = 62.9\%$ to 10.8% and the difference on BW_R^{-3dB} is much decreased from $Y_{BW} = 159.6\%$ to 0.72% . The large discrepancy between results calculated using measured loss factors and manufacturer-provided values is due to the frequency dependence of losses. In Tab. 1, $\delta_{c_{33}^E}$ and $\delta_{\epsilon_{33}^T}$ showed on datasheet are appropriate for low frequency range but will cause overdamping at high frequency, as can be seen in Fig. 9.

	Manufacturer	Measured	Discrepancy
$\delta_{c_{33}^E}$	0.0235	0.0045	80.1%
$\delta_{\beta_{33}^S}$	0.0444	0.0027	93.4%

Table 3. Manufacturer and measured loss factors.

	Experiment	Manufacturer (Y_A)	Meas. (Y_{BW})
A_R (mS)	385.7	143.1 (62.9%)	343.8 (10.8%)
BW_R^{3dB} (kHz)	6.94	18.02 (159.6%)	6.99 (0.72%)

Table 4. EMA discrepancy caused by losses.

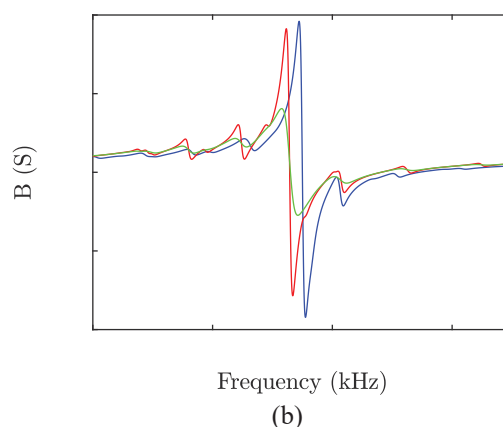
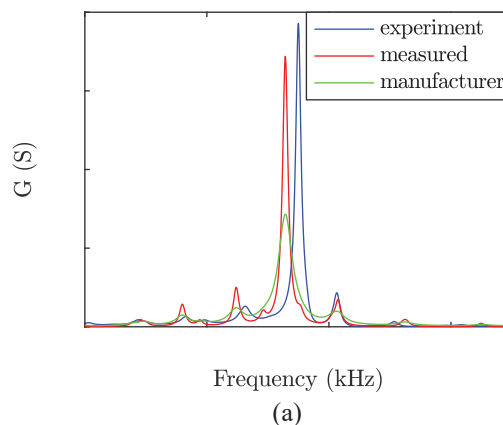


Figure 9. Comparison between experimental and FE model results calculated from measured and manufacturer-provided loss factors: (a) conductance, (b) susceptance.

4.3 Comparison between experimental and FE model results

In this part, experimental results are compared to FE ones. As shown in Fig. 10, the agreement is quite satisfactory. Similar to the results shown in Fig. 3, as delamination ratio Δ increases, the resonance peak becomes shaper and higher (Fig. 10(a)) and A_R or BW_R^{-3dB} changes monotonically with Δ (Fig. 10 (b) and (c)). As we can see from Fig. 10(b) and (c), the evolution of experimental A_R and BW_R^{-3dB} over Δ coincides well with results from FE model and the difference between the three types of delaminations is also confirmed by experiment.

The maximum discrepancy between experimental and numerical values of A_R is 15.71% for “center”, 19.4% for “peripheric” and 16.18% for “wedge” delamination (see Tab. 5). For BW_R^{-3dB} , the maximum discrepancy values are 20.6%, 20.0% and 18.6% respectively for the three types of delaminations (see Tab. 6).

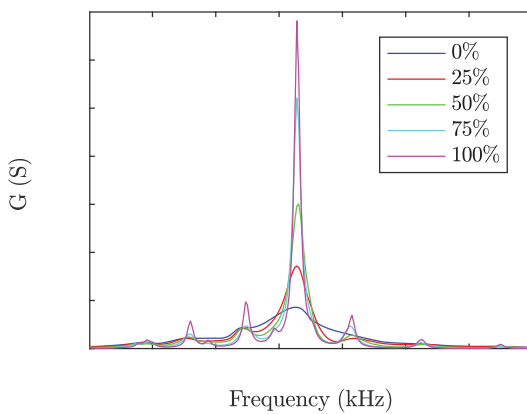
In terms of the impact of delamination ratio on transducer admittance, “center” delamination makes the most, “wedge” delamination less and “peripheric” delamination even less. For example, a 50% FE modeled delamination gives a -3dB bandwidth decrease from 64.98 kHz to 17.42 kHz (73.2%) for “center”, 55.71 kHz (14.3%) for “peripheric” and 31.15 kHz (52.1%) for “wedge”.

Delamination ratio	Center (%)	Peripheric (%)	Wedge (%)
0%	8.8	8.8	8.8
25%	13.91	4.78	16.18
50%	15.71	4.33	13.03
75%	1.38	19.4	1.39
100%	4.87	4.87	4.87

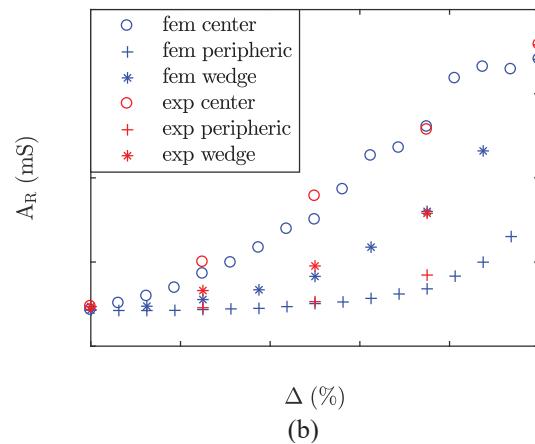
Table 5. Resonance amplitude of thickness mode

Delamination ratio	Center (%)	Peripheric (%)	Wedge (%)
0%	7.9	7.9	7.9
25%	6.84	11.84	6.76
50%	2.68	3.49	14.07
75%	20.57	20.03	18.64
100%	12.15	12.15	12.15

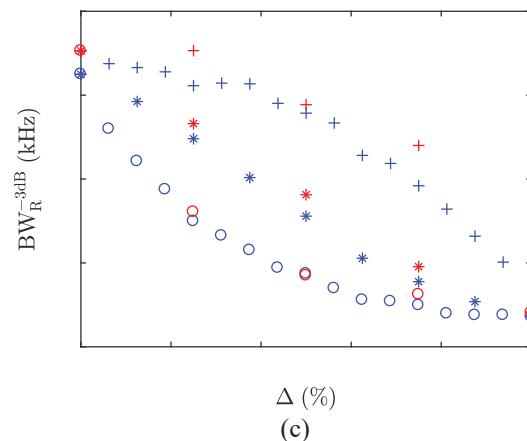
Table 6. -3dB bandwidth of thickness mode



(a)



(b)



(c)

Figure 10. Comparison between results from experiment and FE model: (a) conductance of “center” delamination, (b) resonance amplitude, (c) -3dB bandwidth.

Based on the comprehensive analysis above, we can propose a strategy to reveal the occurrence and extent of a delamination in a transducer during its lifetime:

- 1) determine the change trend of indicators, *i.e.* A_R and BW_R^{-3dB} , through FE modelling;
- 2) validate and adjust the model by experimental measurement, indicators tendency accordingly. The two extreme cases are highly recommended for testing, the 0% (intact) and 100% (no backing);
- 3) monitor and detect the transducer periodically.

The conductance curve allows to intuitively estimate whether a delamination has occurred. Then, the change in A_R and BW_R^{-3dB} provides a quantitative assessment. In addition, two or more measurements make it possible to determine what kind of delamination it is close to.

5. CONCLUSION

A framework for the study of the effect of delamination defects on the performance of ultrasonic transducer is provided. Finite element modelling is used to explore changes in EMA when different kinds of delaminations appear. Numerical results show that the resonance amplitude and bandwidth of thickness mode can particularly reveal the occurrence of a delamination and

indicate its severity and even to a certain extent its kind. Comparison of the results obtained by FE model and experiment shows good agreement.

It has been encouragingly demonstrated that changes in EMA provide possibility for qualitative and quantitative assessment of defects in ultrasonic transducers. Future work will extend this method to a complete structure and to multi-element ultrasonic transducers.

ACKNOWLEDGMENT

The authors are grateful for the financial support from China Scholarship Council (CSC) through the cooperation program UT-INSA (France).

REFERENCES

- [1] W. Kochanski, M. Boeff, Z. Hashemiyani, W. J. Staszewski, and P. K. Verma, "Modelling and numerical simulations of in-air reverberation images for fault detection in medical ultrasonic transducers: A feasibility study," *Journal of Sensors*, vol. 2015, pp. 1–14, 2015.
- [2] M. Martensson, M. Olsson, B. Segall, A. G. Fraser, R. Winter, and L.-A. Brodin, "High incidence of defective ultrasound transducers in use in routine clinical practice," *European Journal of Echocardiography*, vol. 10, pp. 389–394, jan 2009.
- [3] S. D. Pye, W. Ellis, and T. MacGillivray, "Medical ultrasound: a new metric of performance for grey-scale imaging," *Journal of Physics: Conference Series*, vol. 1, pp. 187–192, jan 2004.
- [4] T. Quinn and P. Verma, "The analysis of in-air reverberation patterns from medical ultrasound transducers," *Ultrasound*, vol. 22, pp. 26–36, feb 2014.
- [5] R. Krimholtz, D. A. Leedom, and G. L. Matthaei, "New equivalent circuits for elementary piezoelectric transducers," *Electronics Letters*, vol. 6, no. 13, pp. 398–399, 1970.
- [6] "3d printer filaments." <https://www.raise3d.com>.
- [7] D. H. Torchinsky, J. A. Johnson, and K. A. Nelson, "A direct test of the correlation between elastic parameters and fragility of ten glass formers and their relationship to elastic models of the glass transition," *The Journal of Chemical Physics*, vol. 130, p. 064502, feb 2009.
- [8] "Ferroperm piezoceramic material data for modelling." <https://www.meggittferroperm.com>.
- [9] J. Kocbach, *Finite element modeling of ultrasonic piezoelectric transducers*. PhD thesis, University of Bergen, 2000.
- [10] Y. Zhuang, S. O. Ural, and K. Uchino, "Methodology for characterizing loss factors of piezoelectric ceramics," *Ferroelectrics*, vol. 470, pp. 260–271, oct 2014.
- [11] M. Brissaud, *Matériaux piézoélectriques: caractérisation, modélisation et vibration*. PPUR

presses polytechniques, 2007.